Title

3-Azatetracyclo[5.2.1.15,8.01,5]undecane Derivatives: From Wild-Type Inhibitors of the M2 Ion Channel of Influenza A Virus to Derivatives with Potent Activity against the V27A Mutant

Journal

Journal of Medicinal Chemistry, 56(22)

ISSN

0022-2623

Authors

Rey-Carrizo, Matias
Torres, Eva
Ma, Chunlong
et al.

Publication Date

2013-11-27

DOI

10.1021/jm401340p

Peer reviewed

Published in final edited form as:
J Med Chem. 2013 November 27; 56(22): 9265–9274. doi:10.1021/jm401340p.

3-Azatetracyclo[5.2.1.1^{5,8}.0^{1,5}]undecane derivatives: from wild-type inhibitors of the M2 ion channel of influenza A virus to derivatives with potent activity against the V27A mutant

Matias Rey-Carrizo[ǁ,‡], **Eva Torres**[ǁ,‡], **Chunlong Ma**[#,§], **Marta Barniol-Xicota**[ǁ], **Jun Wang**[†], **Yibing Wu**[†], **Lieve Naesens**[⊥], **William F. DeGrado**[†], **Robert A. Lamb**[§,ʃ], **Lawrence H. Pinto**[#], and **Santiago Vázquez**[*,ǁ]

[ǁ]Laboratori de Química Farmacèutica (Unitat Associada al CSIC), Facultat de Farmàcia, and Institute of Biomedicine (IBUB), Universitat de Barcelona, Av. Joan XXIII s/n, Barcelona E-08028, Spain

[#]Department of Neurobiology and Physiology, Northwestern University, Evanston, Illinois 60208-3500, United States

[†]Department of Pharmaceutical Chemistry, University of California, San Francisco, California 94158, United States

[⊥]Rega Institute for Medical Research, KU Leuven, 3000 Leuven, Belgium

[§]Department of Molecular Biosciences, Northwestern University, Evanston, Illinois 60208-3500, United States

[ʃ]Howard Hughes Medical Institute, Northwestern University, Evanston, Illinois 60208-3500, United States

Abstract

We have synthesized and characterized a series of compounds containing the 3-azatetracyclo[5.2.1.1^{5,8}.0^{1,5}]undecane scaffold designed as analogs of amantadine, an inhibitor of the M2 proton channel of influenza A virus. Inhibition of the wild-type (wt) M2 channel and the amantadine-resistant A/M2-S31N and A/M2-V27A mutant ion channels were measured in *Xenopus* oocytes using two-electrode voltage clamp (TEV) assays. Most of the novel compounds inhibited the wt ion channel in the low micromolar range. Of note, several compounds inhibited the A/M2 V27A mutant ion channel, one of them with submicromolar IC_{50}. None of the compounds was found to inhibit the S31N mutant ion channel. The antiviral activity of three novel dual wt and A/M2-V27A channels inhibitors was confirmed by influenza virus yield assays.

[*]Address correspondence to this author: Tel: +34 934024533.; Fax: +34 934035941. svazquez@ub.edu.
[‡]These authors contributed equally.

Author Contributions

The manuscript was written through contributions of all authors. All authors have given approval to the final version of the manuscript.

Notes

The authors declare no competing financial interest.

Supporting Information. Figure S1 and Table S1 (NMR titration assay). Experimental procedures and characterization data for compounds **12c-d** and **18c-d** to **22c-d**. Table with the elemental analysis data of the new compounds. This material is available free of charge via the Internet at http://pubs.acs.org.

Keywords

Amantadine; cage compounds; influenza A virus; M2 proton channel; drug design

Introduction

The influenza A virus M2 protein is a 97 residues long integral membrane protein with a transmembrane (TM) domain of 19 residues, a small ectodomain of 23 residues, and a 54 residues long cytoplasmic tail.[1] This M2 protein is encoded by a spliced mRNA derived from viral RNA segment 7.[2] The A/M2 proton channel activity is required for viral replication.[3] Influenza A virus particles enter the host cells by endocytosis (mainly via the clathrin-mediated route).[4] Within the endosome, release of the viral ribonucleoprotein (RNPs) complexes from the matrix M1 protein, depends on acidification of the viral interior. This lowering of the pH is accomplished by the M2 proton channel, which facilitates the flow of protons from the acidic endosomal lumen into the interior of the virion.[5] This proton channel function of M2 has been found to be essential in all influenza A subtypes thus far studied. In some virus strains, e.g. H7N1 fowl plague virus, the A/M2 protein also equilibrates the pH of the trans-Golgi network to prevent a premature conformational change of the viral hemagglutinin (HA).[6]

Influenza A viruses are important pathogens which are capable of causing significant morbidity and mortality in humans. Two classes of anti-viral drugs are currently available: the M2 ion channel inhibitors [amantadine (Amt) and rimantadine] and the neuraminidase (NA) inhibitors (oseltamivir and zanamivir).[6] However, the usefulness of Amt and rimantadine dropped sharply in recent years due to the widespread of resistant viruses, which prompted the Centers for Disease Control to recommend discontinuing the use of Amt-based drugs.[7–8] Also, resistance to oseltamivir has been frequently observed in recent flu seasons.[9–10] Therefore, there is an urgent need to develop the next generation of anti-viral drugs that are active against drugresistant influenza viruses. Systematic mutational analysis of the pore-line residues of the A/M2 TM domain identified many Amt-resistance mutations.[11] However, only a few of these mutations (i.e. L26F, V27A, and S31N) have been observed in transmissible viruses, with the S31N mutation being the most frequently occurring Amt-resistance mutation.[12] The channel properties (ion selectivity and activity) of these mutants appear to be very similar to those of the wt M2 channel, suggesting that the channel properties need to be finely tuned in order for the virus to be transmissible.

Many efforts have been made to discover new small molecular inhibitors of Amt-resistant mutant forms of A/M2. For example, Wang et al. reported several spiro compounds, such as **1**-**3**. Spiroadamantane **3** inhibits the L26F and V27A A/M2 mutants with good efficacy in electrophysiological and virus plaque reduction assays.[13–15] Most recently, this group also discovered new compounds, such as **4** and **5**, that inhibit the most prevalent drug-resistant A/M2 mutant, S31N (Chart 1).[16–18]

In this study, we report some novel scaffolds designed to inhibit the A/M2 channel. Several pyrrolidine derivatives were found to inhibit the wt channel as well as the M2-V27A mutant ion channel. The best compound, guanidine **16d**, has a low micromolar activity against the wt channel (IC_{50} = 3.4 μM) and submicromolar activity against the M2-V27A mutant (IC_{50} = 0.29 μM).

Chemistry

During the past years, our group has synthesized several polycyclic Amt analogs containing different scaffolds, including ring-contracted, ring-rearranged and 2,2-dialkyl derivatives of

Amt (Chart 2).[19–22] Several ring-contracted analogs of Amt, such as amines **6** and **7** were evaluated for inhibition of A/M2 proton channel activity, by using the conductance assay in M2-expressing oocytes. They displayed similar IC_{50} values for wt A/M2 as Amt, but, unfortunately, were inactive against the Amt-resistant S31N or V27A mutant forms of A/M2.[20] We have also explored the activity of larger, ring-rearranged analogs of Amt using the pentacyclo[6.4.0.0^{2,10}.0^{3,7}.0^{4,9}]dodecane scaffold. Very interestingly, while primary amines **8** and **9** and several derivatives, including secondary and tertiary amines, amidines and guanidines did not inhibit A/M2 proton channel activity, the conformationally more rigid pyrrolidine-based derivatives **10** and **11** did show a promising activity against the wt A/M2 channel, being only slightly less active than Amt. Moreover, while the primary amines **8** and **9** did not show any activity against the V27A mutant form of A/M2, both pyrrolidine derivatives showed a marginal activity against this mutant (Table 1).[20,22]

Based on these promising results, we reasoned that the synthesis of pyrrolidine analogs of the already active bisnoradamantane **7**, featuring an unprecedented 3-azatetracyclo[5.2.1.1^{5,8}.0^{1,5}]undecane ring, may lead to compounds with higher activity against the wt and the V27A mutant of A/M2.

The reaction of the known[23–24] diacids **12a,b** with urea at 180 °C for 30 minutes yielded imides **13a,b** which were subsequently reduced to give the secondary amines **14a,b** in good overall yields. Reductive alkylation of the secondary amines with formaldehyde and $NaCNBH_3$ led to the corresponding tertiary amines **15a,b** in good yields. Taking into account our observation that some of the corresponding guanidines derived from our previously synthesized amines were also inhibitors of the A/M2 channel,[20] we synthesized guanidines **16a,b** from amines **14a,b** and 1*H*-pyrazole-1-carboxamidine monohydrochloride (Scheme 1).

Recent experimental and computational studies have shown that the mutation of Val27 to a residue with a smaller side chain such as alanine (A/M2-V27A mutant) destroyed the hydrophobic gate formed by this residue and increased the pore radius by ~2 Å at the *N*-terminal end.[14,25–26]

The amine **14a** and guanidine **16a** displayed higher inhibitory activity against the M2-V27A mutant channel than their corresponding smaller analogs, **14b** and **16b** (see below). Also, since recent MD calculations suggested that larger, more hydrophobic molecules may fill the pore of the V27A mutant better,[14] we designed two novel, larger analogs of the dual inhibitor **16a**, i.e. **16c** and **16d**.

For the synthesis of pyrrolidines **14c,d** and **16c,d** following the route outlined in Scheme 1, novel diacid derivatives **12c,d** were required. Thus, we synthesized diacids **12c,d** from easily available diketones **17c,d**, following the synthetic sequence shown in Scheme 2 that we had previously developed for related bisnoradamantane derivatives.[27]

To homologate diketones **17c-d**,[28–30] they were transformed into a mixture of the corresponding *bis*-vinyl iodides *syn*- and *anti*-**19c-d**, *via* the corresponding *bis*-hydrazones, **18c-d**, following the Barton procedure, in 41 and 56%, respectively, overall yield.[31–32] Then, palladium (0) catalyzed methoxycarbonylation of **19c-d** afforded **20c-d** in 62 and 64% yield, respectively, as a mixture of *syn* and *anti* regioisomers. Catalytic hydrogenation (Pd/C) of the mixture of *syn*- and *anti*-**20c-d** gave an stereoisomeric mixture of diesters **21c-d** in 77 and 74% yield, respectively. Reaction of diesters **21c-d** with two equivalents of LiHMDS in anhydrous THF, followed by reaction of the corresponding *bis*-enolate with one equivalent of iodine gave **22c-d** in 47 and 57% yield, respectively. Finally, hydrolysis of diesters **22c-d** gave the diacids **12c-d** in, 63% and 80% yield, respectively (Scheme 2).

From diacids **12c-d**, and following the synthetic sequence shown in Scheme 1, we prepared the amines **14c-d** and the guanidines **16c-d** in good overall yields (see Supporting information for details).

All the pharmacologically evaluated compounds were fully characterized as salts (hydrochlorides or tartrates) through their spectroscopic data and elemental analyses.

Pharmacological activity and structure-activity relationships

Inhibition of wt and Amt-resistant A/M2 ion channels

The inhibitory activity of the compounds was tested on A/M2 channels expressed in *Xenopus* oocytes using the TEV technique. All inhibitors were initially tested at 100 μM; those that inhibited the wt A/M2 channel activity by more than 75% were chosen for measurement of their 50% inhibitory concentration (IC_{50}). The results are given in Table 1.

Amt inhibited wt A/M2 channel with an IC_{50} of 16.0 μM in an isochronic (2 min) inhibition assay. It has been suggested that in designing Amt analogs, pyrrolidine or piperidine derivatives may result in a more favorable orientation inside the M2 channel pore as compared to freely rotating alkylamine chains.[33] Thus, we had previously tested tetracyclic derivatives **8** and **9** and conformationally more rigid amines **10** and **11** (Table 1).[20] In sharp contrast with the poor performance of primary amines **8** and **9**, diene **10** was shown to be able to inhibit wt A/M2 channel by more than 80%, showing an IC_{50} of 33.5 μM. Bis-cyclopropanation slightly increased the potency, since derivative **11** showed an IC_{50} of 24.0 μM. Interestingly, **11** (at a concentration of 100 μM) inhibited the A/M2 V27A channel activity by 17.7%, which is superior to Amt (10.8%), yet much less than **1-3**.[13–15]

Based on these results, we synthesized compounds **14a**, **15a** and **16a**, as conformationally more rigid analogs of **7**. In agreement with the previous trend observed in going from **8** and **9** to **10** and **11**, pyrrolidines **14a** and **16a** were potent inhibitors of the wt channel (IC_{50} of 9.7 and 6.1 μM, respectively) and, very interestingly, were better inhibitors of the V27A mutant channel than **7**, with the guanidine **16a** showing an IC_{50} of 11.4 μM. Alkylation of **14a** to **15a** reduced the inhibitory potency both for the wt and the V27A mutant.

We also synthesized smaller and larger analogs of **14a** and **16a**. As expected, in going from **14a** and **16a** to the smaller analogs **14b** and **16b**, an important reduction of the activity against the V27A mutant was observed, although both compounds kept the inhibitory activity against the wt. Again, the tertiary amine **15b** was less potent than the corresponding secondary amine **14b**. For this reason, no further tertiary amines were synthesized.

In going from the dimethyl derivatives **14a** and **16a** to their corresponding diethyl derivatives, **14c** and **16c**, the activity against both the wt and the V27A mutant channels diminished, probably because the freely rotating ethyl chains of **14c** and **16c** make destabilizing contacts with the backbone of the protein. These contacts should be more evident in the narrower wt channel, as reflected in the lower inhibitory activities of **14c** and **16c** against the wt channel compared to **14a** and **16a**. In the conformationally more rigid amine **14d** and guanidine **16d** the low micromolar inhibitory activity against the wt channel was restored and, pleasingly, good inhibition of the V27A mutant channel was observed, with **16d** showing an IC_{50} of 0.29 μM.

Binding of guanidine 16d

To determine the binding affinity of this class of compounds, we chose one of the most potent inhibitor against wt M2, **16d**, and measured its affinity by solution NMR drug titration. A peptide spanning the transmembrane domain (22–46) of M2, designated as

M2TM, was reconstituted in dodecylphosphocholine (DPC) micelles in a 1:50 peptide to detergent ratio, under which condition M2TM forms tetramer predominantly. **16d** was titrated into the solution and the characteristic peak of W41 $H^{\varepsilon 1}$ was monitored in 1D ^{1}H-NMR (Figure S1). It was found that drug-bound form of M2 is in slow exchange with the apo-form: a new peak at 10.9 ppm, corresponding to W41 $H^{\varepsilon 1}$, emerges upon drug addition and continuously increases with drug titration while the peak at 10.4 ppm associated with the apo-form becomes weaker. Previously, we observed that this peak correlates with the binding of drugs to the pore of the channel.[34] A plot of the peak integral at 10.9 ppm against increasing drug concentrations is shown in Figure 1. The data were fitted using the nonlinear least-squares fitting equation as described earlier.[34] The best fit gave a stoichiometry ratio of 1.37 ± 0.28 drug per tetramer and a dissociation constant K_d of 40 ± 24 μM. It should be noted that the titration was conducted at a protein concentration (1.6 mM) that is significantly above K_d, thus the actual K_d is difficult to be determined. However, theoretical curve fittings with fixed stoichiometry (N=1, meaning one drug per tetramer binding) and different K_d (4 μM, 100 μM, and 400 μM) showed the K_d to be significantly less than 100 μM (see Figure 1).

It is worth noting that the difference between the IC_{50} and K_d reflects the differences in the experimental assays used to determine these properties. It has long been known that M2 channel blockers are very slow binders, as noted in the second order rate constant of amantadine (i.e., 600 to 900 $M^{-1}s^{-1}$ for the Udorn strain).[35] So, the IC_{50} depends on the amount of time the drug is exposed to the target.

Antiviral activity and cytotoxicity in cell culture

All novel compounds were subjected to antiviral evaluation against a wide range of DNA and RNA viruses, using CPE reduction assays in relevant cell lines. None of the compounds displayed activity against the enveloped DNA viruses herpes simplex virus (type 1 or type 2) or vaccinia virus; the enveloped RNA viruses feline coronavirus, parainfluenza-3 virus, respiratory syncytial virus, vesicular stomatitis virus, Sindbis virus or Punta Toro virus; or the non-enveloped RNA viruses Coxsackievirus B4 and Reovirus-1 (data not shown).

In our basic CPE reduction assays with influenza virus, performed in MDCK cell cultures, three virus strains were used: the A/PR/8/34 strain, an A/H1N1 virus with two amantadine-resistance mutations (S31N and V27T) in the A/M2 protein; the A/HK/7/87 strain, which has a wt A/M2 protein, and the B/HK/5/72 strain. The antiviral data obtained by microscopic scoring of the virus-induced CPE were confirmed by the colorimetric MTS cell viability assay. In parallel, the compounds were applied to uninfected MDCK cells to estimate the cytotoxicity by microscopy or MTS cell viability assay (Table 2).

In agreement with the TEV assays (see above), all the compounds were not active against the amantadine-resistant A/PR/8/34 strain that carries the M2-S31N mutation. For compounds **14a**, **14b** and Amt, a correlation was seen between their cell culture activities for the A/HK/7/87 virus (EC_{50} values: 1.6 μM for **14a** and 7.9 μM for **14b**) and their IC_{50} values against A/M2 wt proton channel function. This was, however, not the case for the amine **14d** and for the guanidines **16a,b,d**. These four compounds had quite pronounced cytotoxicity in the MDCK cells in our three-day CPE reduction assay (i.e. minimum cytotoxic concentrations of 8 μM or lower), and this may have masked the potential inhibitory effect of the compounds towards the A/HK/7/87 virus (Table 2).

It is difficult to speculate on the cause of the toxicity. These are amphiphilic compounds that might well cause a membrane disrupting effect given sufficient time of exposure. The CPE test is a 3-day assay and, hence, some compounds may display toxic effects that make it

impossible to assess the potential antiviral effect. On the other hand, compounds with favorable activity and selectivity are easily identified in the CPE assay, i.e. **14a** and **14b**.

We therefore evaluated amine **14d** and the guanidines **16a,b,d** in a virus yield assay with strain A/HK/7/87 (carrying a wt A/M2), in which the virus released in the supernatant at 24 hours after infection was quantified by real-time RT-PCR.[36] As shown in Table 3, amine **14d** and guanidines **16a** and **16d** had an EC_{90} value (i.e. concentration causing 10-fold reduction in virus yield) below 1 μM, which is the same order of magnitude as the values noted for Amt and rimantadine. Of these, **16a** and Amt were able to afford a 100-fold reduction in virus yield, with EC_{99} values of ~1 μM.

Conclusions

The present works showed that, starting from compounds active against the wt A/M2 channel it is possible to design compounds active against both the wt and the V27A mutant A/M2 channels. In fact, some of them inhibit both channels more effectively than amantadine inhibits the wt. The low micromolar antiviral activity of the three dual inhibitors identified, amine **14d** and guanidines **16a** and **16d**, was confirmed by an influenza virus yield assay. Interestingly, the compounds reported here are the first examples of non-adamantane derivatives endowed with low micromolar activity against the V27A/M2 mutant channel, opening the way to the design of novel M2 inhibitors structurally based on non-adamantane scaffolds. Taking into account the broad utility of the adamantane scaffold in medicinal chemistry, the novel azapolycyclic ring reported here may be of interest for other therapeutic areas where the adamantane derivatives are of medicinal interest.

Experimental Section

Plasmid, mRNA synthesis, and microinjection of oocytes

The cDNA encoding the influenza A/Udorn/72 (A/M2) was inserted into pGEM3 vector for the expression on oocyte plasma membrane. A/M2 S31N and A/M2 V27A mutants were generated by QuikChange site-directed mutagenesis kit (Agilent Technologies). The synthesis of mRNA and microinjection of oocytes have been described previously.[37]

Two-electrode voltage clamp analysis

Macroscopic membrane current was recorded 48–72 hours after injection as described previously.[13] The tested compounds were applied at pH 5.5 at various concentrations when the inward current reaches maximum. The compounds were applied for 2 min, and residual membrane current was compared with the membrane current before the application of compounds. Membrane currents were analyzed with pCLAMP 10.0 software package (Axon Instruments, Sunnyvale, CA).

NMR of drug titration

The M2TM peptide corresponding to the transmembrane domain of the Udorn M2, SSDPLVVAASIIGILHLILWILDRL, was synthesized using an optimized protocol as described before.[34] The NMR sample was prepared starting from mixing peptide and DPC in the desired molar ratio in ethanol, followed by removal of ethanol by nitrogen flush and lyphilization to ensure completely removal. The resulting film was dissolved in NMR buffer consisting of 50 mM sodium phosphate in 10% D_2O and 90% H_2O, pH 7.5. Drug, **16d**, was dissolved in H_2O and added to the NMR sample gradually. The final dilution was less than 2%.

Cell culture assays for antiviral activity and cytotoxicity

The antiviral activity of the compounds was determined in established CPE reduction assays, using a diverse set of DNA and RNA viruses as indicated, and including three (sub)types of influenza virus: A/Puerto Rico/8/34 (A/H1N1); A/Hong Kong/7/87 (A/H3N2) and B/Hong Kong/5/72.[38–39] Briefly, Madin-Darby canine kidney cells seeded in 96-well plates were exposed to influenza virus [multiplicity of infection: 50 $CCID_{50}$ (50% cell culture infective dose) per well] together with the test compounds. After three days incubation at 35 °C, microscopy was performed to score the virus-induced cytopathic effect (CPE) as well as compound cytotoxicity. These data were confirmed by the colorimetric formazan-based MTS cell viability assay. Antiviral activity was expressed as the EC_{50} value, or compound concentration producing 50% inhibition of the virus-induced CPE, as determined by microscopy or MTS assay. Compound cytotoxicity was expressed as the minimum inhibitory concentration (MCC), i.e. the concentration producing minimal changes in cell morphology, or the CC_{50} value, i.e. the concentration causing 50% reduction in cell viability by MTS assay.

To determine the effect of the compounds on virus yield, MDCK cells were incubated with influenza virus (strain A/HongKong/7/87) and compounds as above. After 24 hr incubation the supernatants were collected and frozen. The virus released in these supernatants was quantified by real-time qRT-PCR, as described.[36] Antiviral activity was expressed as the EC_{90} or EC_{99} value, i.e. the compound concentration producing a virus yield reduction of 1 $\log_{10}$ or 2 $\log_{10}$, respectively.

Chemical Synthesis. General Methods

Melting points were determined in open capillary tubes with a MFB 595010M Gallenkamp melting point apparatus. 300 MHz ^{1}H/75.4 MHz ^{13}C NMR spectra, 400 MHz ^{1}H/100.6 MHz ^{13}C NMR spectra, and 500 MHz ^{1}H NMR spectra were recorded on Varian Gemini 300, Varian Mercury 400, and Varian Inova 500 spectrometers, respectively. The chemical shifts are reported in ppm (δ scale) relative to internal tetramethylsilane, and coupling constants are reported in Hertz (Hz). Assignments given for the NMR spectra of the new compounds have been carried out on the basis of DEPT, COSY $^{1}H/^{1}H$ (standard procedures), and COSY $^{1}H/^{13}C$ (gHSQC and gHMBC sequences) experiments. An asterisk (*) in the NMR data means interchangeable signals. IR spectra were run on a Perkin-Elmer Spectrum RX I spectrophotometer. Absorption values are expressed as wave-numbers (cm^{-1}); only significant absorption bands are given. The GC/MS analysis was carried out in an inert Agilent Technologies 5975 gas chromatograph equipped with an Agilent 122-5532 DB-5MS 1b (30 m × 0.25 mm) capillary column with a stationary phase of phenylmethylsilicon (5% diphenyl – 95% dimethylpolysiloxane), using the following conditions: initial temperature of 50 °C (1 min), with a gradient of 10 °C/min up to 300 °C, and a temperature in the source of 250 °C. *Solvent Delay* (SD) of 4 minutes and a pressure of 7,35 psi. Column chromatography was performed on silica gel 60 A C.C (35–70 mesh, SDS, ref 2000027). Thin-layer chromatography was performed with aluminum-backed sheets with silica gel 60 F_{254} (Merck, ref 1.05554), and spots were visualized with UV light and 1% aqueous solution of $KMnO_4$. The analytical samples of all of the new compounds which were subjected to pharmacological evaluation possessed a purity ≥95% as evidenced by their elemental analyses.

7,8-Dimethyl-3-azatetracyclo[5.2.1.1^{5,8}.0^{1,5}]undeca-2,4-dione (13a)—A mixture of known[23] diacid **12a** (3.0 g, 13.4 mmol) and urea (4.2 g, 95% purity, 67.0 mmol) was heated slowly to 135 °C. When the mixture melted it was heated to 180 °C for 30 min and cooled. Water (66 mL) was added and the suspension was extracted with CH_2Cl_2 (6×40 mL). The combined organic extracts were washed with brine (1×45 mL), dried with

anhydrous Na_2SO_4, filtered and concentrated in vacuo to dryness to give imide **13a** as a white solid (2.07 g, 75% yield). An analytical sample of **13a** was obtained by crystallization from $CHCl_3$, mp 209–210 °C; IR (KBr) ν 3194 (N-H), 1766 and 1711 (C=O st) cm^{-1}; ^1H NMR (400 MHz, $CDCl_3$) δ 1.23 [s, 6 H, C7(8)-C$\underline{H}_3$], 1.88 [dd, J = 9.8 Hz, J' = 1.9 Hz, 4 H, 6(9,10,11)-H_α], 1.92 [dd, J = 9.8 Hz, J' = 2.0 Hz, 4 H, 6(9,10,11)-H_β], 8.24 (bs, 1 H, NH); ^{13}C NMR (100.6 MHz, $CDCl_3$) δ 16.1 [CH_3, C7(8)-CH_3], 51.8 [C, C7(8)], 55.2 [CH_2, C6(9,10,11)], 57.5 [(C, C1(5)], 177.4 (C, CO). GC/MS (EI), m/e (%): 205 ($M^{\cdot+}$, 4), 134 (83), 120 (100), 119 (53), 150 (48), 117 (10), 105 (17), 92 (22), 91 (38), 79 (15), 77 (23). HRMS-ESI+ m/z [M+H]$^+$ calcd for [$C_{12}H_{15}NO_2$+H]$^+$: 206.1176, found: 206.1185.

7,8-Dimethyl-3-azatetracyclo[5.2.1.1^{5,8}.0^{1,5}]undecane hydrochloride (14a•HCl)—To a stirred solution of imide **13a** (0.36 g, 1.8 mmol) in anhydrous toluene (8 mL) at 0 °C, sodium bis-(2-methoxyethoxy)aluminium hydride (2.7 mL, 65% in toluene, 8.8 mmol) was added dropwise. When the addition was finished, the solution was heated under reflux for 72 h. The mixture was cooled to 0 °C (ice-water bath), treated with 30% aq solution of KOH til basic pH and stirred at room temperature for 1 h. The organic layer was separated and the aqueous one was extracted with CH_2Cl_2 (3×15 mL). The combined organic layers were dried with anhydrous Na_2SO_4, filtered and evaporated in vacuo. The obtained solid residue was dissolved in Et_2O (20 mL) and treated with excess of HCl in Et_2O to give the hydrochloride of **14a** (0.41 g, 99% yield) as a solid that was collected by filtration. An analytical sample of **14a•HCl** was obtained as a white solid by crystallization from MeOH/Et_2O, mp 248–249 °C; IR (KBr) ν 3527, 2953, 2883, 2767, 2702, 2588, 2536, 2413, 2241, 1902, 1610, 1594, 1508, 1483, 1457, 1444, 1379, 1363, 1297, 1260, 1183, 983, 871 cm^{-1}; ^1H NMR (400 MHz, CD_3OD) δ 1.19 [s, 6 H, C7(8)-CH_3], 1.67 [m, 8 H, 6(9,10,11)-H_2], 3.26 [bs, 4 H, C2(4)-H_2]; ^{13}C NMR (100.6 MHz, CD_3OD) δ 16.7 [CH_3, C7(8)-CH_3], 47.5 [CH_2, C2(4)], 52.4 [C, C7(8)], 56.6 [CH_2, C6(9,10,11)], 58.7 [C, C1(5)]. MS (EI), m/e (%): 177 ($M^{\cdot+}$, 6), 135 (21), 134 ($C_{10}H_{14}^{\cdot+}$, 100), 133 (35), 122 (29), 119 (22), 107 (22), 106 (35), 105 (48), 93 (32), 92 (21), 91 (64), 80 (23), 79 (24), 77 (34), 55 (21).

3,7,8-Trimethyl-3-azatetracyclo[5.2.1.1^{5,8}.0^{1,5}]undecane hydrochloride (15a•HCl)—To a suspension of **14a** (0.5 g, 2.4 mmol) in acetonitrile (10 mL), $NaBH_3CN$ (95% content, 0.46 g, 6.9 mmol), AcOH (0.4 mL) and formaldehyde (37% aqueous solution 0.6 mL, 7.3 mmol) were added and the mixture was magnetically stirred at room temperature for 8 h. Then, more $NaBH_3CN$ (95% content, 0.46 g, 6.9 mmol) and formaldehyde (37% aqueous solution 0.6 mL, 7.3 mmol) were added and stirring at room temperature was continued for 18 h more. The mixture was concentrated in vacuo, the residue was suspended in water (20 mL) and the solution was made basic with aqueous solution of 2 N NaOH (4 mL) and extracted with EtOAc (3×20 mL). The combined organic extracts were dried (anhydrous Na_2SO_4), filtered, treated with an excess of an ethereal solution of HCl and concentrated in vacuo to give the hydrochloride of **15a** (0.4 g, 73% yield) as a white solid. An analytical sample of **15a•HCl** was obtained by crystallization from 2-propanol, mp 280–281 °C (dec.); IR (KBr) ν 3384, 3007, 2953, 2882, 2591, 2564, 2474, 2449, 1644, 1480, 1462, 1446, 1419, 1378, 1349, 1293, 1257, 1248, 1193, 1173, 1123, 1105, 1068, 1025, 967, 893 cm^{-1}; ^1H NMR (500 MHz, $CDCl_3$) δ 1.09 (s, 3 H) and 1.11 (s, 3 H) (C7-CH_3 and C8-CH_3), 1.47 [d, J = 8.5 Hz, 2 H, 9(11)-H_α], 1.52 [dd, J = 7.2 Hz, J' = 2.0 Hz, 2 H, 6(10)-H_β], 1.63 [d, J = 8.0 Hz, 2 H, 6(10)-H_α], 2.18 [dd, J = 8.0 Hz, J = 2.0 Hz, 2 H, 9(11)-H_β], 2.79 [m, 2 H, C2(4)-H_a], 2.82 (d, J = 3.5 Hz, 3 H, N-CH_3), 3.64 [d, J = 7.5 Hz, 2 H, C2(4)-H_b] and 12.65 (bs, 1H, NH); ^{13}C NMR (125.7 MHz, $CDCl_3$) δ 16.0 (CH_3) and 16.2 (CH_3) (C7-CH_3) and (C8-CH_3), 40.7 (CH_3, N-CH_3), 50.2 (C, C7),* 51.9 (C, C8),* 54.7 [CH_2, C9(11)],* 56.3 [CH_2, C6(10)],* 56.5 [CH_2, C2(4)], 57.2 [C, C1(5)]. MS (EI), m/e (%): 191 ($M^{\cdot+}$, 43), 190 (40), 148 (100), 136 (35), 134 (32), 133 (31), 107 (22), 106 (28), 105 (28), 94 (20), 91 (41), 77 (21), 58 (50), 57 (37).

3-Amidino-7,8-dimethyl-3-azatetracyclo[5.2.1.1^{5,8}.0^{1,5}]undecane hydrochloride (16a•HCl)—A suspension of **14a•HCl** (0.37 g, 1.73 mmol), Et_3N (0.44 mL, 2.79 mmol) and 1*H*-pyrazole-1-carboxamidine hydrochloride (0.31 g, 2.11 mmol) in CH_3CN (5 mL) was heated at 70 °C for 6 h. Then, the suspension was allowed to stand overnight in the freezer (4 °C) and the solid was separated by filtration in vacuo and washed with diethyl ether to give **16a•HCl** as a beige solid (450 mg, 61% yield), mp 276–277 °C (dec). IR (KBr) ν 3295, 3093, 2937, 2876, 2723, 1634, 1531, 1478, 1456, 1361, 1293, 1189, 1161, 1133, 1116, 1045, 955, 737, 604, 540 cm^{-1}; ^{1}H NMR (400 MHz, CD_3OD) δ 1.18 [s, 6 H, C7(8)-CH_3], 1.63 [d, *J* = 6.9 Hz, 4 H, 6(9,10,11)-H_α], 1.69 [d, *J* = 6.9 Hz, 4 H, 6(9,10,11)-H_β], 3.49 [s, 4 H, C2(4)-H_2]; ^{13}C NMR (100.6 MHz, CD_3OD) δ 16.7 [CH_3, C7(8)-CH_3], 49.5 [CH_2, C2(4)], 52.3 [C, C7(8)], 58.0 [CH_2, C6(9,10,11)], 58.4 [C, C1(5)], 156.7 (C, C=N). MS (EI), m/e (%): 220 (54), 219 ($M^{\cdot+}$, 41), 166 (66), 165 (100), 164 (68), 163 (23), 145 (33), 134 ($C_{10}H_{14}^{\cdot+}$, 29), 133 (21), 123 (23), 122 (26), 120 (23), 119 (24), 114 (26), 113 (34), 112 (24), 107 (23), 106 (29), 105 (65), 91 (58), 79 (22), 77 (31), 74 (41), 73 (51), 72 (23).

3-azatetracyclo[5.2.1.1^{5,8}.0^{1,5}]undeca-2,4-dione (13b)—From known[24] diacid **12b** (0.5 g, 2.6 mmol) and urea (0.8 g, 95% purity, 12.7 mmol) and following the same procedure as reported for **13a**, imide **13b** was obtained as a white solid (0.33 g, 73% yield). An analytical sample of **13b** was obtained by crystallization from CH_2Cl_2, mp 131–132 °C; IR (KBr) ν 3189 (N-H), 1749 and 1715 (C=O st), 1346, 1135, 1054, 833 cm^{-1}; ^{1}H NMR (400 MHz, $CDCl_3$) δ 1.85 [dd, *J* = 9.6 Hz, *J′* = 2.4 Hz, 4 H, 6(9,10,11)-H_α], 2.05 [dd, *J* = 7.6 Hz, *J′* = 1.6 Hz, 4 H, 6(9,10,11)-H_β], 2.68 [m, 2 H, 7(8)-H], 7.74 (bs, 1 H, NH); ^{13}C NMR (100.6 MHz, $CDCl_3$) δ 40.3 [CH, C7(8)], 49.5 [CH_2, C6(9,10,11)], 57.1 [C, C1(5)], 176.8 (C, C=O). GC/MS (EI), m/e (%): 177 ($M^{\cdot+}$, 3), 106 (100), 105 (21), 93 (13), 92 (22), 91 (39), 79 (10), 78 (22), 77 (12), 65 (16). HRMS-ESI− m/z [*M*−H]$^-$ calcd for [$C_{10}H_{11}NO_2$−H]$^-$: 176.0717, found: 176.0725.

3-azatetracyclo[5.2.1.1^{5,8}.0^{1,5}]undecane hydrochloride (14b•HCl)—To a stirred solution of imide **13b** (0.41 g, 2.3 mmol) in anhydrous THF (15 mL) at 0 °C, $LiAlH_4$ (0.9 g, 23.1 mmol) was added portionwise. When the addition was finished, the solution was heated under reflux for 72 h. The mixture was cooled to 0 °C (ice-water bath), treated with 10 N aq solution of NaOH til basic pH (8 mL) and stirred at room temperature for 1 h. The mixture was filtered through Celite® and the filtrate was thoroughly washed with CH_2Cl_2. The organic layer was separated, dried with anhydrous Na_2SO_4, filtered and evaporated in vacuo. The obtained solid residue was dissolved in Et_2O (20 mL) and treated with excess of HCl in Et_2O to give the hydrochloride of **14b** (0.32 g, 75% yield). An analytical sample of **14b•HCl** was obtained as a white solid by crystallization from MeOH/Et_2O, mp 218–219 °C; IR (KBr) ν 3421, 2989, 2961, 2887, 2739, 2530, 2493, 1560, 1481, 1458, 1450, 1420, 1388, 1353, 1294, 1248, 1228, 1115, 1082, 1007, 988, 949, 924, 901, 881, 853, 771, 657, 604, 495 cm^{-1}; ^{1}H NMR (400 MHz, CD_3OD) δ 1.60 [broad d, *J* = 7.6 Hz, 4 H, 6(9,10,11)-H_α], 1.76 [dd, *J* = 7.6 Hz, *J′* = 2.0 Hz, 4 H, 6(9,10,11)-H_β], 2.48 [m, 2 H, 7(8)-H], 3.32 [bs, 4 H, C2(4)-H_2]; ^{13}C NMR (100.6 MHz, CD_3OD) δ 41.3 [CH, C7(8)], 47.0 [CH_2, C2(4)], 50.2 [CH_2, C6(9,10,11)], 58.3 [C, C1(5)]. MS (EI), m/e (%): 149 ($M^{\cdot+}$, 29), 108 (53), 107 ($C_8H_{11}^+$, 100), 106 (29), 105 (30), 95 (31), 94 (86), 92 (26), 91 (46), 80 (27), 79 (62), 77 (37), 71 (21), 70 (20).

3-Methyl-3-azatetracyclo[5.2.1.1^{5,8}.0^{1,5}]undecane hydrochloride (15b•HCl)—To a suspension of **14b** (0.32 g, 2.1 mmol) in acetonitrile (13 mL), $NaBH_3CN$ (95% content, 0.28 g, 4.3 mmol), AcOH (1.2 mL) and formaldehyde (37% aqueous solution, 1.1 mL, 14.1 mmol) were added and the mixture was magnetically stirred at room temperature for 8 h. Then, more $NaBH_3CN$ (95% content, 0.28 g, 4.3 mmol) and formaldehyde (37% aqueous

solution 1.1 mL, 14.1 mmol) were added and stirring at room temperature was continued for 18 h more. The mixture was concentrated in vacuo, the residue was suspended in water (20 mL) and the solution was made basic with aqueous solution of 2 N NaOH (4 mL) and extracted with EtOAc (3×25 mL). The combined organic extracts were dried (anhydrous Na_2SO_4), filtered, treated with an excess of an ethereal solution of HCl and concentrated in vacuo to give the hydrochloride of **15b** (0.24 g, 70% yield) as a white solid. An analytical sample of **15b•HCl** was obtained by crystallization from MeOH/Et_2O, mp 223–224 °C (dec.); IR (KBr) ν 3003, 2962, 2889, 2572, 2462, 1628, 1508, 1482, 1465, 1349, 1293, 1269, 1228, 1177, 1129, 1106, 1079, 1060, 965, 890 cm^{-1}; ^1H NMR (400 MHz, CD_3OD) δ 1.61 (dd, J = 8.2 Hz, J' = 3.3 Hz, 2 H), 1.60–1.73 (complex signal, 4 H) and 1.79 (dd, J = 8.5 Hz, J = 2.4 Hz, 2H) [C6(10)-H_2 and C9(11)-H_2], 2.46 [m, 2H, C7(8)-H], 2.96 (s, 3H, N-CH_3), 3.18 (d, J = 12.0 Hz, 2 H) and 3.70 [d, J = 12.0 Hz, 2 H) [C2(4)-H_2]; ^{13}C NMR (100.6 MHz, CD_3OD) δ 39.9 [CH, C7(8)], 40.7 (CH_3, N-CH_3), 41.7 [CH, C7(8)], 49.7 [CH_2, C9(11)],* 50.5 [CH_2, C6(10)]*, 57.3 [CH_2, C2(4)], 58.0 [C, C1(5)]. MS (EI), m/e (%): 163 ($M^{\cdot+}$, 57), 162 (100), 121 (26), 120 (35), 108 (30), 105 (11), 94 (13), 91 (19), 79 (17), 77 (14), 58 (22). HRMS-ESI+ m/z [M+H]$^+$ calcd for [$C_{11}H_{17}N$+H]$^+$: 164.1434, found: 164.1432.

3-Amidino-3-azatetracyclo[5.2.1.1^{5,8}.0^{1,5}]undecane hydrochloride (16b•HCl)— From a suspension of **14b•HCl** (0.13 g, 0.7 mmol), Et_3N (0.17 mL, 1.08 mmol) and 1*H*-pyrazole-1-carboxamidine hydrochloride (0.12 g, 0.8 mmol) in CH_3CN (5 mL) and following the same procedure as reported for **16a•HCl**, guanidine **16b•HCl** was obtained as a beige solid (150 mg, 96% yield), mp 254–255 °C (dec) (CH_2Cl_2). IR (KBr) ν 3401, 3323, 3153, 2981, 2966, 2933, 2886, 1652, 1635, 1615, 1471, 1456, 1373, 1297, 1196, 1085, 565 cm^{-1}; ^1H NMR (400 MHz, CD_3OD) δ 1.55 [broad d, J = 7.2 Hz, 4 H, 6(9,10,11)-H_α], and 1.79 [broad d, J = 8.8 Hz, 4 H, 6(9,10,11)-H_β], 2.44 [s, 2 H, C7(8)], 3.55 [s, 4 H, C2(4)-H_2]; ^{13}C NMR (100.6 MHz, CD_3OD) δ 41.2 [CH, C7(8)], 48.9 [CH_2, C2(4)], 51.5 [CH_2, C6(9,10,11)], 57.8 [C, C1(5)], 156.7 (C, C=NH). MS (EI), m/e (%): 194 (43), 193 (40), 192 [(M+H)$^+$, 14], 153 (22), 152 (84), 151 (67), 150 (28), 139 (100), 138 (62), 117 (44), 115 (53), 114 (35), 109 (27), 108 (29), 107 (53), 106 (29), 105 (23), 96 (32), 95 (54), 94 (26), 92 (25), 91 (73), 81 (25), 80 (24), 79 (54), 78 (28), 77 (65), 75 (32), 74 (23), 71 (20), 65 (24), 63 (25), 53 (26). Anal. Calcd. for $C_{11}H_{17}N_3$·HCl (227.73): C 58.01, H 7.97, N 18.45. HRMS-ESI+ m/z [M+H]$^+$ calcd for [$C_{11}H_{17}N_3$+H]$^+$: 192.1495, found: 192.1494.

7,8-Diethyl-3-azatetracyclo[5.2.1.1^{5,8}.0^{1,5}]undeca-2,4-dione (13c)—From diacid **12c** (1.12 g, 4.44 mmol) and urea (1.33 g, 22.2 mmol) and following the same procedure as reported for **13a**, imide **13c** was obtained as a white solid (0.91 g, 87% yield). An analytical sample of **13b** was obtained by crystallization from CH_2Cl_2/*n*-pentane, mp 204–205 °C; IR (KBr) ν 3404, 3198, 3072, 2962, 1761, 1707, 1464, 1353, 1210, 1143, 1061, 830, 725, 618, 506 cm^{-1}; ^1H NMR (400 MHz, $CDCl_3$) δ 0.92 [t, J = 7.6 Hz, 6 H, C7(8)-$CH_2C\underline{H}_3$], 1.63 [q, J = 7.6 Hz, 4 H, C7(8)-$C\underline{H}_2CH_3$], 1.80 [broad d, J = 7.2 Hz, 4 H, 6(9,10,11)-H_a], 1.96 [broad d, J = 7.2 Hz, 4 H, 6(9,10,11)-H_b], 8.13 (broad s, 1H, NH); ^{13}C NMR (100.6 MHz, $CDCl_3$) δ 10.0 [CH_3, C7(8)-$CH_2\underline{C}H_3$], 22.8 [CH_2, C7(8)-$\underline{C}H_2CH_3$], 52.1 [CH_2, C6(9,10,11)], 56.6 [C, C7(8)], 57.2 [C, C1(5)], 177.7 (C, CO). GC/MS, m/z (%); main ions: 233 ($M^{\cdot+}$, 34), 163 (16), 162 (96), 148 (100), 147 (20), 133 (80), 106 (18), 105 (35), 91 (40), 77 (16). HRMS-ESI+ m/z [M+H]$^+$ calcd for [$C_{14}H_{19}NO_2$+H]$^+$: 234.1489, found: 234.1499.

7,8-Diethyl-3-azatetracyclo[5.2.1.1^{5,8}.0^{1,5}]undecane (2*R*,3*R*)-tartrate, [14c•(2*R*, 3*R*)- tartrate]—To a stirred solution of imide **13c** (907 mg, 3.89 mmol) in anhydrous toluene (32 mL) at 0 °C, sodium bis-(2-methoxyethoxy)aluminium hydride (5.95 mL, 65% solution in toluene, 5.95 mmol) was added dropwise. When the addition was finished, the solution was heated under reflux for 72 h. The mixture was cooled to 0 °C (ice-water bath),

treated with 30% aq solution of KOH til basic pH and stirred at room temperature for 1 h. The organic layer was separated and the aqueous one was extracted with CH_2Cl_2 (3×30 mL). The combined organic layers were dried with anhydrous Na_2SO_4, filtered and evaporated in vacuo to give amine **14c** as an orange oil (326 mg). The amine was dissolved in methanol (5 mL) and treated with (2*R*,3*R*)-tartaric acid (170 mg, 1.13 mmol) dissolved in the minimum amount of methanol. The mixture was concentrated in vacuo to yield **14c** as its (2*R*,3*R*)-tartrate as a yellow solid (459 mg, 33% yield). An analytical sample of **14c•(2*R*, 3*R*)-tartrate** was obtained by crystallization from MeOH/Et_2O, mp 165–166 °C. IR (KBr) ν 3422, 3321, 2958, 2882, 1718, 1585, 1455, 1407, 1303, 1263, 1210, 1130, 1068, 899, 834, 784, 680, 618 cm^{-1}; ^1H NMR (400 MHz, CD_3OD) δ 0.93 [t, *J* = 7.6 Hz, 6 H, C7(8)-$CH_2C\underline{H}_3$], 1.53 [broad d, *J* = 7.2 Hz, 4 H, 6(9,10,11)-H_a], 1.61 [q, *J* = 7.6 Hz, 4 H, C7(8)-$C\underline{H}_2CH_3$], 1.76 [broad d, *J* = 7.2 Hz, 4 H, 6(9,10,11)-H_b], 3.27 [s, 4 H, 2(4)-H2], 4.39 [s, 2 H, C<u>H</u>(OH)-CO_2H]; ^{13}C NMR (100.6 MHz, CD_3OD) δ 10.5 [CH_3, C7(8)-$CH_2\underline{C}H_3$], 24.2 [CH_2, C7(8)-$\underline{C}H_2CH_3$], 47.6 [CH_2, C2(4)], 53.3 [CH_2, C6(9,10,11)], 57.9 [C, C1(5)]*, 58.0 [C, C7(8)]*, 74.4 [CH, <u>C</u>H(OH)], 177.6 (C, CO_2H). GC/MS, m/z (%); main ions: 205 [$(C_{14}H_{23}N)^{\cdot+}$, 7], 190 (11), 176 (16), 163 (21), 162 (100), 161 (14), 147 (27), 136 (20), 133 (21), 120 (15), 119 (21), 107 (15), 105 (23), 91 (37).

3-Amidino-7,8-diethyl-3-azatetracyclo[5.2.1.1^{5,8}.0^{1,5}]undecane hydrochloride (16c•HCl)—From a suspension of **14c•HCl** (459 mg, 1.29 mmol), Et_3N (0.30 mL, 2.06 mmol) and 1*H*-pyrazole-1-carboxamidine hydrochloride (226 mg, 1.54 mmol) in CH_3CN (10 mL) and following the same procedure as reported for **16a•HCl**, guanidine **16c•HCl** was obtained as a yellow solid (242 mg, 76% yield). An analytical sample was obtained by crystallization from *t*-butanol, mp 231–232 °C (dec). IR (KBr) ν 3291, 3220, 3173, 3102, 2957, 2877, 2364, 2337, 1603, 1556, 1455, 1369, 1290, 1112, 1077, 946, 899, 677 cm^{-1}; ^1H NMR (400 MHz, CD_3OD) δ 0.93 [t, *J* = 7.6 Hz, 6 H, C7(8)-$CH_2C\underline{H}_3$], 1.58 [broad d, *J* = 6.6 Hz, 4 H, 6(9,10,11)-H_a], 1.61 [q, *J* = 7.6 Hz, 4 H, C7(8)-$C\underline{H}_2CH_3$], 1.72 [broad d, *J* = 6.6 Hz, 4 H, 6(9,10,11)-H_b], 3.51 [s, 4 H, 2(4)-H]; ^{13}C NMR (100.6 MHz, CD_3OD) δ 10.5 [CH_3, C7(8)-$CH_2\underline{C}H_3$], 24.2 [CH_2, C7(8)-$\underline{C}H_2CH_3$], 49.8 [CH_2, C2(4)], 54.6 [CH_2, C6(9,10,11)], 57.5 [C, C1(5)]*, 57.9 [C, C7(8)]*, 156.7(C, C=NH). MS, m/z (%); main ions: 247 ($C_{15}H_{25}N_3^{\cdot+}$, 34), 246 (26), 232 (100), 192 (33), 178 (33), 177 (20), 162 (18), 159 (14), 119 (28), 112 (24), 105 (20), 91 (35), 79 (15), 72 (68).

12-Azapentacyclo[6.5.1.1^{3,10}.0^{1,10}.0^{3,8}]pentadeca-11,13-dione (13d)—From diacid **12d** (520 mg, 2.10 mmol) and urea (624 mg, 10.4 mmol) and following the same procedure as reported for **13a**, imide **13d** was obtained as a white solid (400 mg, 83% yield). An analytical sample of **13d** was obtained by crystallization from CH_2Cl_2/*n*-pentane, mp 202–203 °C; IR (ATR) ν 3404, 3189, 3079, 2934, 1758, 1706, 1473, 1396, 1354, 1213, 1140, 1061, 840, 733, 618 cm^{-1}; ^1H NMR (400 MHz, $CDCl_3$) δ 1.58 [m, 4 H, 5(6)-H_2], 1.70 [m, 4 H, 4(7)-H_2], 1.83 [d, *J* = 7.2 H, 4 H, 2(9,14,15)-H_a], 1.99 [d, *J* = 7.2 Hz, 4 H, 2(9,14,15)-H_b], 8.09 [broad s, 1 H, N<u>H</u>]; ^{13}C NMR (100.6 MHz, $CDCl_3$) δ 18.7 [CH_2, C5(6)], 25.5 [CH_2, C4(7)], 52.2 [C, C3(8)], 53.0 [CH_2, C2(9,14,15)], 56.9 [C, C1(10)], 177.5 [C, C11(13)]. MS, m/z (%); main ions: 231 ($M^{\cdot+}$, 27), 160 (23), 146 (100), 145 (49), 131 (15), 118 (21), 117 (35), 91 (31). HRMS-ESI+ m/z [*M*+H]$^+$ calcd for $[C_{14}H_{17}NO_2+NH_4]^+$: 249.1598, found: 249.1607.

12-Azapentacyclo[6.5.1.1^{3,10}.0^{1,10}.0^{3,8}]pentadecane (2*R*,3*R*)-tartrate, [14d•(2*R*, 3*R*)-tartrate]—From imide **13d** (378 mg, 1.51 mmol) in dry toluene (14 mL) and sodium bis-(2-methoxyethoxy)aluminium hydride (2.30 mL, 65% solution in toluene, 7.55 mmol) and following the same procedure as reported for **14c•(2*R*,3*R*)-tartrate**, amine **14d** as its (2*R*,3*R*)-tartrate was obtained as a pale yellow solid (442 mg, 83% yield). An analytical sample of **14d•(2*R*,3*R*)-tartrate** was obtained by crystallization from CH_2Cl_2/CH_3OH, mp

124–125 °C. IR (KBr) ν 3377, 2931, 2542, 2360, 1715, 1585, 1475, 1450, 1351, 1296, 1118, 1069, 983, 897, 834, 690 cm^{-1}; ^1H NMR (400 MHz, CD_3OD) δ 1.57–1.72 [complex signal, 12 H, 5(6)-H_2, 4(7)-H_2 and 2(9,14,15)-H_a], 1.75 [broad d, J = 6.8 Hz, 4 H, 2(9,14,15)-H_b], 3.27 [s, 4 H, 11(13)-H_2], 4.36 [s, 2 H, C<u>H</u>(OH)-CO_2H]; ^{13}C NMR (100.6 MHz, CD_3OD) δ 20.0 [CH_2, C5(6)], 26.8 [CH_2, C4(7)], 47.3 [CH_2, C11(13)], 52.9 [C, C3(8)], 54.3 [CH_2, C2(9,14,15)], 58.2 [C, C3(8)], 74.7 (CH, <u>C</u>H(OH)], 178.2 (C, CO_2H). GC/MS, m/z (%); main ions: 203 [$(C_{14}H_{21}N)^{\cdot+}$, 62], 202 (43), 188 (100), 175 (21), 160 (39), 148 (77), 146 (28), 134 (95), 133 (43), 132 (34), 131 (33), 121 (79), 120 (36), 119 (26), 118 (23), 117 (40), 106 (24), 105 (29), 94 (19), 93 (19), 92 (20), 91 (79), 82 (26), 80 (29), 79 (29), 77 (30), 70 (29). HRMS-ESI+ m/z [*M*+H]$^+$ calcd for $[C_{14}H_{21}N+H]^+$: 204.1747, found: 204.1748.

12-Amidino-12-azapentacyclo[6.5.1.1^{3,10}.0^{1,10}.0^{3,8}]pentadecane hydrochloride (16d•HCl)—From a suspension of **14d** (249 mg, 1.22 mmol), Et_3N (0.14 mL, 0.98 mmol) and 1*H*-pyrazole-1-carboxamidine hydrochloride (215 mg, 1.47 mmol) in CH_3CN (9.5 mL) and following the same procedure as reported for **16a•HCl**, guanidine **16d•HCl** was obtained as a yellow solid (215 mg, 63% yield). An analytical sample was obtained by crystallization from *t*-butanol, mp 254–255 °C (dec). IR (ATR) ν 3303, 3178, 2926, 2871, 2371, 1647, 1616, 1464, 1361, 1293, 1127, 1035, 958, 929, 775, 701, 609, 559 cm^{-1}; ^1H NMR (400 MHz, CD_3OD) δ 1.55–1.65 [complex signal, 8 H, 5(6)-H_2 and 2(9,14,15)-H_a], 1.69 [m, 4 H, 4(7)-H_2], 1.80 [broad d, *J* = 6.8 Hz, 4 H, 2(9,14,15)-H_b], 3.50 [s, 4 H, 11(13)-H_2]; ^{13}C NMR (100.6 MHz, CD_3OD) δ 20.0 [CH_2, C5(6)], 26.8 [CH_2, C4(7)], 49.4 [CH_2, C11(13)], 52.8 [C, C3(8)], 55.6 [CH_2, C2(9,14,15)], 57.8 [CH_2, C1(10)], 156.7 (C, CN). MS, m/z (%); main ions: 245 [$(C_{15}H_{23}N_3)^{\cdot+}$, 91], 230 (39), 217 (72), 190 (100), 171 (21), 162 (58), 148 (38), 143 (23), 131 (31), 129 (25), 120 (30), 117 (27), 112 (56), 111 (27), 105 (27), 91 (69), 79 (29), 77 (32), 72 (39), 60 (30).

Supplementary Material

Refer to Web version on PubMed Central for supplementary material.

Acknowledgments

ET and SV thank the Spanish Ministerio de Ciencia e Innovación (FPU fellowship to ET; grant CTQ2011-22433 to SV) and the Generalitat de Catalunya (grant SCG-2009-294) for financial support. MRC thanks the Govern d'Andorra for a PhD grant. LN acknowledges financial support from the Geconcerteerde Onderzoeksacties (GOA/10/014), and the technical assistance from W. van Dam. WFD acknowledges support from GM56423 from the NIH.

ABBREVIATIONS

Amt	amantadine
BSA	bovine serum albumin
CD	circular dichroism
DMEM	Dulbecco's modified eagle medium
DMPC	dimyristoylphosphatidylcholine
DPC	dodecylphosphocholine
LiHMDS	Lithium bis(trimethylsilyl)amide
MDCK	Madin-Darby Canine Kidney
MD	molecular dynamics

MTS	3-(4,5-dimethylthiazol-2-yl)-5-(3-carboxymethoxyphenyl)-2-(4-sulfophenyl)-2*H*-tetrazolium
NMR	Nuclear Magnetic Resonance
PBS	phosphate buffered saline
TEV	two-electrode voltage clamps
TM	transmembrane
wt	wild-type

References

1. Lamb RA, Zebedee SL, Richardson CD. Influenza virus M2 protein is an integral membrane protein expressed on the infected-cell surface. Cell. 1985; 40:627–633. [PubMed: 3882238]
2. Lamb RA, Lai CJ, Choppin PW. Sequences of mRNAs derived from genome RNA segment 7 of influenza virus: colinear and interrupted mRNAs code for overlapping proteins. Proc Natl Acad Sci USA. 1981; 78:4170–4174. [PubMed: 6945577]
3. Takeda M, Pekosz A, Shuck K, Pinto LH, Lamb RA. Influenza a virus M2 ion channel activity is essential for efficient replication in tissue culture. J Virol. 2002; 76:1391–1399. [PubMed: 11773413]
4. Vanderlinden E, Naesens L. Emerging antiviral strategies to interfere with influenza virus entry. Med Res Rev. 2013; 3310.1002/med.21289
5. Zhirnov OP. Solubilization of matrix protein M1/M from virions occurs at different pH for orthomyxo- and paramyxoviruses. Virology. 1990; 176:274–279. [PubMed: 2158693]
6. Grambas S, Hay AJ. Maturation of influenza A virus hemagglutinin–estimates of the pH encountered during transport and its regulation by the M2 protein. Virology. 1992; 190:11–18. [PubMed: 1529523]
7. Bright RA, Shay DK, Shu B, Cox NJ, Klimov AI. Adamantane resistance among influenza A viruses isolated early during the 2005–2006 influenza season in the United States. JAMA. 2006; 295:891–894. [PubMed: 16456087]
8. Fiore AE, Shay DK, Haber P, Iskander JK, Uyeki TM, Mootrey G, Bresee JS, Cox NJ. Prevention and control of influenza. Recommendations of the Advisory Committee on Immunization Practices (ACIP), 2007. MMWR Recomm Rep. 2007; 56:1–54. [PubMed: 17625497]
9. Moscona A. Global transmission of oseltamivir-resistant influenza. N Engl J Med. 2009; 360:953–956. [PubMed: 19258250]
10. Baz M, Abed Y, Papenburg J, Bouhy X, Hamelin ME, Boivin G. Emergence of oseltamivir-resistant pandemic H1N1 virus during prophylaxis. N Engl J Med. 2009; 361:2296–2297. [PubMed: 19907034]
11. Balannik V, Carnevale V, Fiorin G, Levine BG, Lamb RA, Klein ML, DeGrado WF, Pinto LH. Functional studies and modeling of pore-lining residue mutants of the influenza a virus M2 ion channel. Biochemistry. 2010; 49:696–708. [PubMed: 20028125]
12. Furuse Y, Suzuki A, Oshitani H. Large-scale sequence analysis of M gene of influenza A viruses from different species: mechanisms for emergence and spread of amantadine resistance. Antimicrob Agents Chemother. 2009; 53:4457–4463. [PubMed: 19651904]
13. Balannik V, Wang J, Ohigashi Y, Jing X, Magavern E, Lamb RA, DeGrado WF, Pinto LH. Design and pharmacological characterization of inhibitors of amantadine-resistant mutants of the M2 ion channel of influenza A virus. Biochemistry. 2009; 48:11872–11882. [PubMed: 19905033]
14. Wang J, Ma C, Fiorin G, Carnevale V, Wang T, Hu F, Lamb RA, Pinto LH, Hong M, Klein ML, DeGrado WF. Molecular dynamics simulation directed rational design of inhibitors targeting drug-resistant mutants of influenza A virus M2. J Am Chem Soc. 2011; 133:12834–12841. [PubMed: 21744829]

15. Wang J, Ma C, Wu Y, Lamb RA, Pinto LH, DeGrado WF. Exploring organosilane amines as potent inhibitors and structural probes of influenza A virus M2 proton channel. J Am Chem Soc. 2011; 133:13844–13847. [PubMed: 21819109]
16. Wang J, Wu Y, Ma C, Fiorin G, Wang J, Pinto LH, Lamb RA, Klein ML, DeGrado WF. Structure and inhibition of the drug-resistant S31N mutant of the M2 ion channel of influenza A virus. Proc Natl Acad Sci USA. 2013; 110:1315–1320. [PubMed: 23302696]
17. Wang J, Ma C, Wang J, Jo H, Canturk B, Fiorin G, Pinto LH, Lamb RA, Klein ML, DeGrado WF. Discovery of Novel Dual Inhibitors of the Wild-Type and the Most Prevalent Drug-Resistant Mutant, S31N, of the M2 Proton Channel from Influenza A Virus. J Med Chem. 2013; 56:2804–2812. [PubMed: 23437766]
18. Williams JK, Tietze D, Wang J, Wu Y, DeGrado WF, Hong M. Drug-induced conformational and dynamical changes of the S31N mutant of the influenza M2 proton channel investigated by solid-state NMR. J Am Chem Soc. 2013; 135:9885–9897. [PubMed: 23758317]
19. Camps P, Duque MD, Vázquez S, Naesens L, De Clercq E, Sureda FS, López-Querol M, Camins A, Pallàs M, Prathalingam SR, Kelly JM, Romero V, Ivorra D, Cortés D. Synthesis and pharmacological evaluation of several ring-contracted amantadine analogs. Bioorg Med Chem. 2008; 16:9925–9936. [PubMed: 18954995]
20. Duque MD, Ma C, Torres E, Wang J, Naesens L, Juárez-Jiménez J, Camps P, Luque FJ, DeGrado WF, Lamb RA, Pinto LH, Vázquez S. Exploring the size limit of templates for inhibitors of the M2 ion channel of influenza A virus. J Med Chem. 2011; 54:2646–2657. [PubMed: 21466220]
21. Torres E, Vanderlinden E, Fernández R, Miquet S, Font-Bardia M, Naesens L, Vázquez S. Synthesis and anti-influenza activity of 2,2-dialkylamantadines and related compounds. ACS Med Chem Lett. 2012; 3:1065–1069.
22. Torres E, Duque MD, Vanderlinden E, Ma C, Pinto LH, Camps P, Froeyen M, Vázquez S, Naesens L. Role of the viral hemagglutinin in the anti-influenza virus activity of newly synthesized polycyclic amine compounds. Antiviral Res. 2013; 99:281–291. [PubMed: 23800838]
23. Camps P, Font-Bardia M, Pérez F, Solans X, Vázquez S. Synthesis, chemical trapping and dimerization of 3,7-dimethyltricyclo[3.3.0.$0^{3,7}$]oct-1(5)-ene: [2+2] retrocycloaddition of the cyclobutane dimer. Angew Chem, Int Ed Engl. 1995; 34:912–914.
24. Camps P, Luque FJ, Orozco M, Pérez F, Vázquez S. Synthesis, chemical trapping and dimerization of tricyclo[3.3.0.$0^{3,7}$]oct-1(5)-ene, the consummate member of a series of pyramidalized alkenes. Tetrahedron Lett. 1996; 37:8605–8608.
25. Pielak RM, Chou JJ. Solution NMR structure of the V27A drug resistant mutant of influenza A M2 channel. Biochem Biophys Res Commun. 2010; 401:58–63. [PubMed: 20833142]
26. Gu RX, Liu LA, Wang YH, Xu Q, Wei DH. Structural comparison of the wild-type and drug-resistant mutants of the influenza A M2 proton channel by molecular dynamics simulations. J Phys Chem B. 2013; 117:6042–6051. [PubMed: 23594107]
27. Ayats C, Camps P, Duque MD, Font-Bardia M, Muñoz MR, Solans X, Vázquez S. Alternative syntheses of the new D_{2d} symmetric tetramethyl tricyclo[3.3.0.$0^{3,7}$]octane-1,3,5,7-tetracarboxylate. J Org Chem. 2003; 68:8715–8718. [PubMed: 14575509]
28. Makhseed S, McKeown NB. Novel spiro-polymers with enhanced solubility. Chem Commun. 1999:255–256.
29. Weiss U, Edwards JM. A one-step synthesis of ketonic compounds of the petalane [3.3.3]and -[4.3.3]propellane series. Tetrahedron Lett. 1968; 47:4885–4887.
30. Bertz, SH.; Cook, JM.; Gawish, A.; Weiss, U. Organic Syntheses. Vol. VII. Wiley; New York: 1990. Condensation of dimethyl 1,3-acetonedicarboxylate with 1,2-dicarbonyl compounds: *cis*-bicyclo[3.3.0]octane-3,7-diones; p. 50-59.Collect
31. Barton DHR, Bashiardes G, Fourrey JL. Studies on the oxidation of hydrazones with iodine and with phenylselenenyl bromide in the presence of strong organic bases; an improved procedure for the synthesis of vinyl iodides and phenyl-vinyl selenides. Tetrahedron. 1988; 44:147–162.
32. Barton, DHR.; Chen, M.; Jaszberenyi, JCs; Taylor, DK. Organic Syntheses. Vol. IX. Wiley; New York: 1998. Preparation and reactions of 2-*tert*-butyl-1,1,3,3-tetramethylguanidine: 2,2,6-trimethylcyclohexen-1-yl iodide; p. 147-150.Collect

33. Kolocouris A, Spearpoint P, Martin SR, Hay AJ, López-Querol M, Sureda FX, Padalko E, Neyts J, De Clercq E. Comparisons of the influenza virus A M2 channel binding affinities, anti-influenza virus potencies and NMDA antagonistic activities of 2-alkyl-2-aminoadamantanes and analogues. Bioorg Med Chem Lett. 2008; 18:6156–6160. [PubMed: 18947998]

34. Cady SD, Wang J, Wu Y, DeGrado WF, Hong M. Specific binding of adamantane drugs and direction of their polar amines in the pore of the influenza M2 transmembrane domain in lipid bilayers and dodecylphosphocholine micelles determined by NMR Spectroscopy. J Am Chem Soc. 2011; 133:4274–4284. [PubMed: 21381693]

35. Wang C, Takeuchi K, Pinto LH, Lamb RA. Ion channel activity of influenza A virus M2 protein: characterization of the amantadine block. J Virol. 1993; 67:5585–5594. [PubMed: 7688826]

36. Stevaert A, Dallocchio R, Dessì A, Pala N, Rogolino D, Sechi M, Naesens L. Mutational analysis of the binding pockets of the diketo acid inhibitor L-742, 001 in the influenza virus PA endonuclease. J Virol. 2013; 87:10524–10538. [PubMed: 23824822]

37. Ma C, Soto CS, Ohigashi Y, Taylor A, Bournas V, Glawe B, Udo MK, DeGrado WF, Lamb RA, Pinto LH. Identification of the pore-lining residues of the BM2 ion channel protein of influenza B virus. J Biol Chem. 2008; 283:15921–15931. [PubMed: 18408016]

38. Vanderlinden E, Göktas F, Cesur Z, Froeyen M, Reed ML, Russell CJ, Cesur N, Naesens L. Novel inhibitors of influenza virus fusion: structure-activity relationship and interaction with the viral hemagglutinin. J Virol. 2010; 84:4277–4288. [PubMed: 20181685]

39. Naesens L, Vanderlinden E, Roth E, Jeko J, Andrei G, Snoeck R, Pannecouque C, Illyes E, Batta G, Herczegh P, Sztaricskai F. Anti-influenza virus activity and structure-activity relationship of aglycoristocetin derivatives with cyclobutenedione carrying hydrophobic chains. Antiviral Res. 2009; 82:89–94. [PubMed: 19200809]

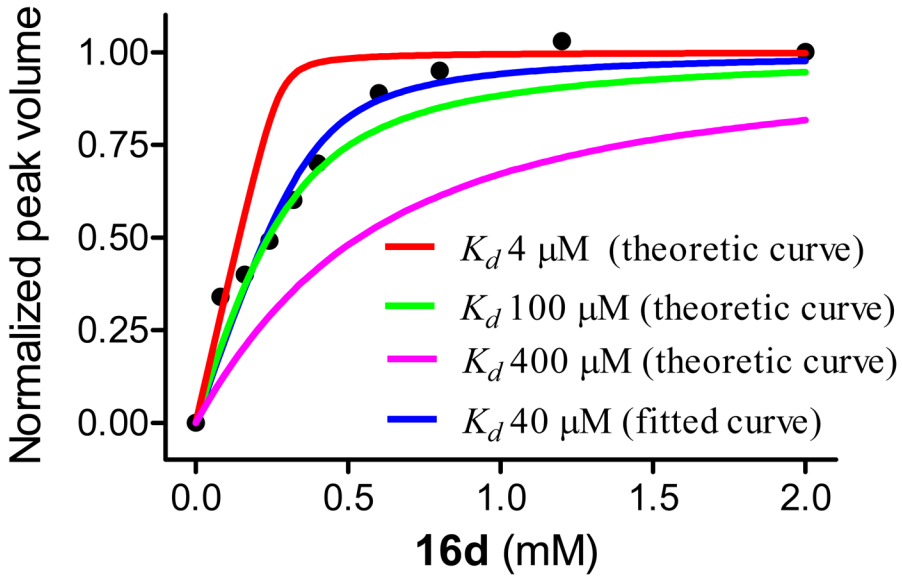

Figure 1.

Binding affinity of **16d** to wt M2TM as determined by solution NMR drug titration. Normalized peak volume of the W41 $H^{\varepsilon 1}$ in the drug-bound form was plotted as a function of **16d** concentration. The fitting yields a stoichiometry ratio of 1.37 ± 0.28 drug/tetramer with a K_d of 40 ± 24 μM (curve shown in blue). In comparison, theoretical curve fittings with fixed stoichiometry (N=1) and K_d of 4 μM, 100 μM and 400 μM are shown in red, green, and pink, respectively. Details about curve fitting can be found in the Supporting Information.

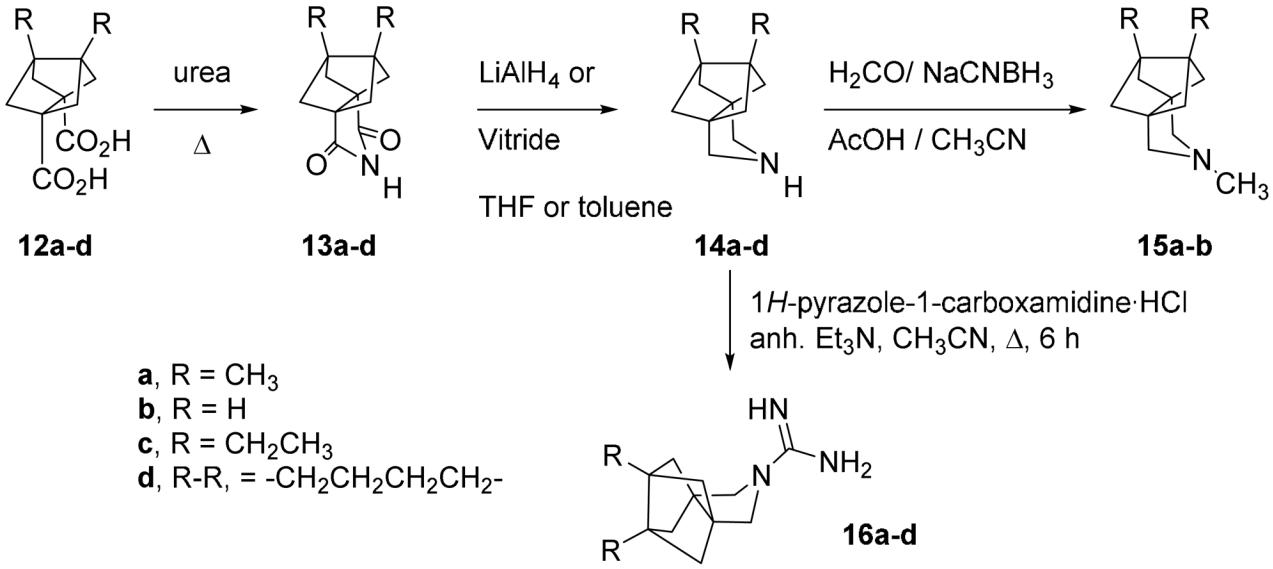

Scheme 1.
Synthesis of polycyclic pyrrolidine derivatives.

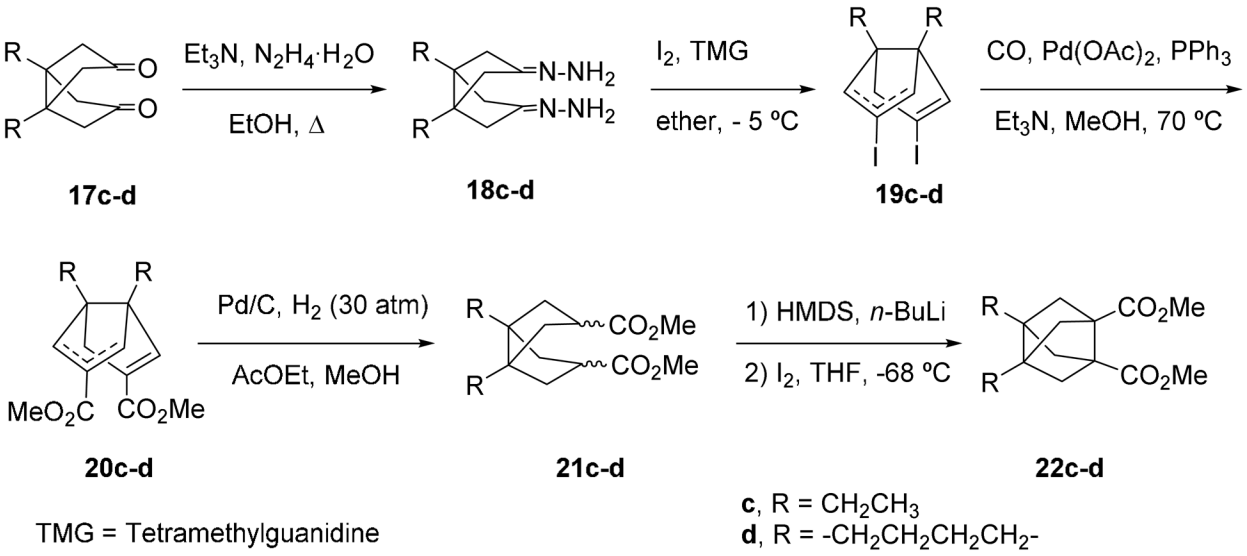

Scheme 2.
Synthesis of diesters **22c-d**.

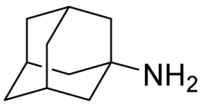

amantadine
A/M2 wt IC_{50} = 16.1 μM
A/M2 V27A IC_{50} > 500 μM
A/M2 S31N IC_{50} = 200 μM

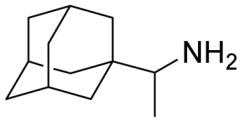

rimantadine
A/M2 wt IC_{50} = 10.8 μM
A/M2 V27A IC_{50} > 500 μM
A/M2 S31N IC_{50} > 500 μM

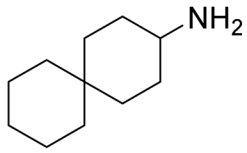

1
A/M2 wt IC_{50} = 12.6 μM
A/M2 V27A IC_{50} = 84.9 μM

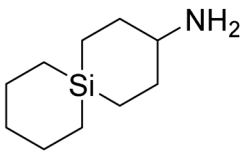

2
A/M2 wt IC_{50} = 14 μM
A/M2 V27A IC_{50} = 31 μM

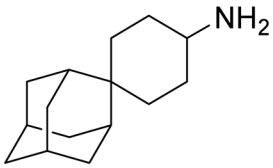

3
A/M2 wt IC_{50} = 19 μM
A/M2 V27A IC_{50} = 0.3 μM
A/M2 S31N IC_{50} > 100 μM

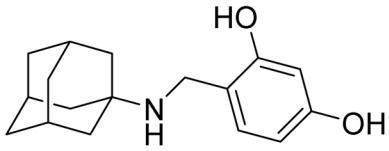

4
A/M2 wt IC_{50} = 59 μM
A/M2 V27A IC_{50} > 100 μM
A/M2 S31N IC_{50} = 35.2 μM

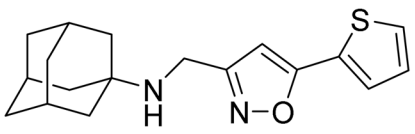

5
A/M2 wt IC_{50} > 100 μM
A/M2 V27A IC_{50} > 100 μM
A/M2 S31N IC_{50} = 16 μM

Chart 1.
Structures of amantadine, rimantadine and recently developed analogs with potent activity against mutant A/M2 channels. The IC_{50} values shown are reported 50% inhibitory concentrations obtained in the TEV assay.[13–18]

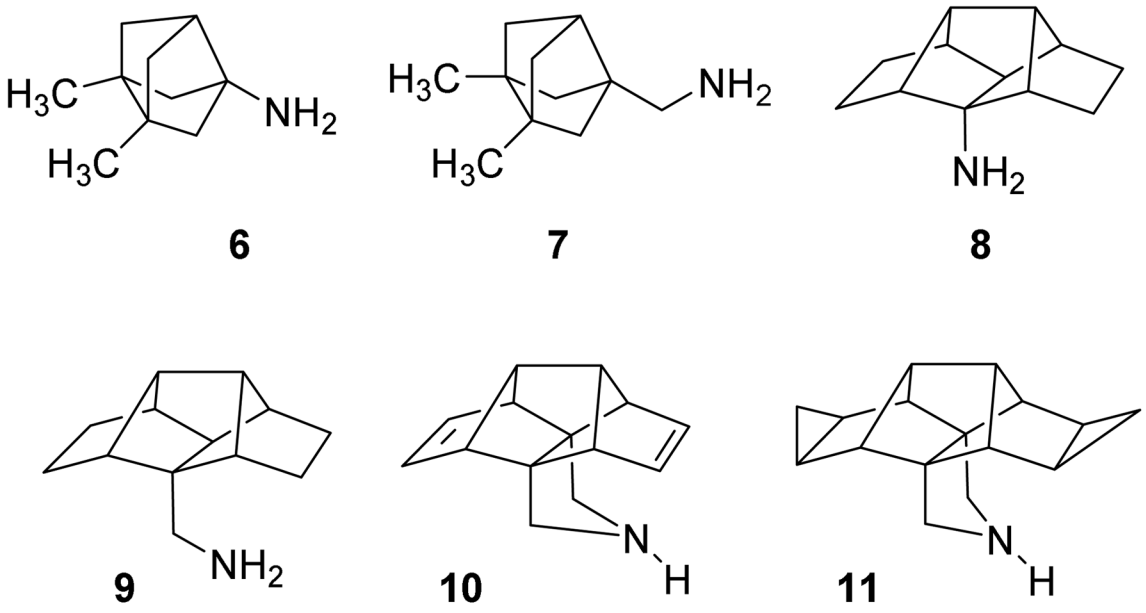

Chart 2.
Structures of known ring-contracted and ring-rearranged analogs of amantadine.

Table 1

Inhibitory effect of the synthesized compounds on A/M2 wt, S31N or V27A proton channel functions.[a]

Compound	A/M2 wt (mean ± SE)		A/M2 S31N (mean ± SE)		A/M2 V27A (mean ± SE)	
	Inhibition by 100 μM for 2 min (%)	IC_{50} (μM)	Inhibition by 100 μM for 2 min (%)	IC_{50} (μM)	Inhibition by 100 μM for 2 min (%)	IC_{50} (μM)
Amantadine	91.0 ± 2.1	16.0 ± 1.2	35.6 ± 1.5	199.9 ± 13.5	10.8 ± 2.0	ND
6	93.6 ± 0.9	17.0 ± 1.0	22.1 ± 0.2	252.2 ± 13.2	10.6 ± 0.7	ND
7	97.3 ± 0.4	7.2 ± 0.3	0	ND	17.6 ± 1.8	ND
8	4.8 ± 2.8	ND	0	ND	0	ND
9	12.8 ± 1.0	ND	0	ND	0	ND
10	82.5 ± 0.8	33.5 ± 1.6	0	ND	9.2 ± 1.0	ND
11	86.5 ± 0.8	24.0 ± 2.1	0	ND	17.7 ± 0.5	ND
14a	93.8 ± 0.8	9.7	0	ND	26.0 ± 0.3	ND
15a	87.9 ± 0.6	16.3	0	ND	12.3 ± 1.6	ND
16a	92.4 ± 0.6	6.1	1.0 ± 1.0	ND	84.2 ± 1.0	11.4
14b	93.9 ± 0.2	11.7	6.2 ± 0.7	ND	5.6 ± 1.5	ND
15b	88.3 ± 0.2	25.2	0	ND	0	ND
16b	95.7 ± 1.5	1.05	0	ND	0	ND
14c	65.0 ± 1.7	ND	13.1 ± 1.7	ND	15.8 ± 2.7	ND
16c	42.8 ± 1.8	ND	10.8 ± 1.2	ND	79.2 ± 0.4	13.8
14d	85.3 ± 0.8	4.5	11.9 ± 1.0	ND	76.2 ± 0.3	20.5
16d	93.1 ± 2.5	3.4	5.7 ± 2.0	ND	93.8 ± 0.9	0.29

ND, Not Determined.

[a] Isochronic (2 min) values for IC_{50} are given. See text and experimental section for details.

Table 2

Antiviral activity in influenza virus-infected MDCK[a] cells.

Compound	Antiviral EC_{50}[b] (μM)						Cytotoxicity (μM) at 72 hr	
	Influenza A/H1N1		Influenza A/H3N2		Influenza B		CC_{50}[c]	MCC[d]
	CPE	MTS	CPE	MTS	CPE	MTS		
14a	>100	>100	1.6	>100	>100	>100	59	100
15a	>100	>100	>100	>100	>100	>100	49	≥20
16a	>100	>100	>100	>100	>100	>100	1.4	4
14b	>100	>100	7.9	7.2	>100	>100	≥59	100
15b	>100	>100	>100	>100	>100	>100	>100	≥100
16b	>50	>50	>50	>50	>50	>50	10	8.5
14c	>100	>100	>100	>100	>100	>100	49	20
16c	>100	>100	>100	>100	>100	>100	6.2	4.0
14d	>100	>100	>100	>100	>100	>100	6.8	4.0
16d	>100	>100	>100	>100	>100	>100	3.1	4.0
Amantadine	34	38	0.84	0.82	>500	>500	>500	>500
Rimantadine	18	4.3	0.62	0.12	>500	>500	203	500

[a] MDCK: Madin-Darby canine kidney cells.

[b] Virus strains: A/PR/8/34 (A/H1N1); A/HK/7/87 (A/H3N2) and B/HK/5/72. The EC_{50} represents the 50% effective concentration, or compound concentration producing 50% inhibition of virus replication, as determined by microscopic scoring of the CPE at 72 hr post infection, or by the MTS cell viability test.

[c] MCC: minimum cytotoxic concentration, or concentration producing minimal alterations in cell morphology after 72 hr incubation with compound.

[d] CC_{50}: 50% cytotoxic concentration, as determined by the MTS cell viability test. Values shown are the mean of 2–3 determinations.

Table 3

Activity of guanidine compounds in influenza virus yield assay.

Compound	Activity[a] (μM) against A/HK/7/87		Cytotoxicity at 24 hr
	EC_{90} (μM)	EC_{99} (μM)	MCC (μM)[b]
16a	0.46	0.79	>50
16b	20	≥38	>50
14d	0.85	>10	>50
16d	0.37	>2	≥10
Amt	0.22	1.1	≥500
Rimantadine	0.10	>4	≥500
Ribavirin	4.6	11	>100

[a] Antiviral activity was determined by a qRT-PCR based virus yield assay to quantify the virus in the supernatant at 24 post infection.[35] EC_{90} and EC_{99}: concentrations causing 1 $\log_{10}$ and 2 $\log_{10}$ reduction in virus yield, respectively.

[b] MCC: minimum cytotoxic concentration, or concentration producing minimal alterations in cell morphology after 24 hr incubation with compound.